Geophysical Research Letters

RESEARCH LETTER
10.1029/2020GL091900

Key Points:

- Sea spray aerosol production is sensitive to sea spray aerosol radiative forcing via an atmosphere-ocean feedback
- The Southern Hemisphere near-surface westerly jet is sensitive to sea spray aerosol radiative forcing
- Sea spray aerosol impacts on surface climate depend on the sea spray aerosol source function used by a climate model

Supporting Information:

- Supporting Information S1

Correspondence to:
L. E. Revell,
laura.revell@canterbury.ac.nz

Citation:
Revell, L. E., Wotherspoon, N. E., Jones, O. J., Bhatti, Y. A., Williams, J. H. T., Mackie, S. L., & Mulcahy, J. P. (2021). Atmosphere-ocean feedback from wind-driven sea spray aerosol production. *Geophysical Research Letters*, *48*, e2020GL091900. https://doi.org/10.1029/2020GL091900

Received 30 AUG 2020
Accepted 11 MAR 2021

Atmosphere-Ocean Feedback From Wind-Driven Sea Spray Aerosol Production

L. E. Revell[1], N. E. Wotherspoon[1], O. J. Jones[1], Y. A. Bhatti[1], J. H. T. Williams[2], S. L. Mackie[3], and J. P. Mulcahy[4]

[1]School of Physical and Chemical Sciences, University of Canterbury, Christchurch, New Zealand, [2]National Institute of Water and Atmospheric Research, Wellington, New Zealand, [3]Department of Physics, University of Otago, Dunedin, New Zealand, [4]Met Office, Exeter, UK

Abstract Marine aerosol production is influenced by wind speed, particularly over the Southern Ocean which is the windiest region on Earth year-round. Using climate model simulations with artificially enhanced sea spray aerosol (SSA), we show that Southern Ocean wind speeds are sensitive to SSA via surface cooling resulting from enhanced aerosol concentrations. The near-surface westerly jet weakens, therefore reducing SSA production. Comparing coupled and atmosphere-only simulations indicates that SSA partially regulates its own production via a feedback between the atmosphere and ocean. The decrease in radiative forcing in the coupled model is approximately one-quarter of that simulated by the atmosphere-only model, and the extent of the feedback also depends on the SSA source function used. Our results highlight the importance of understanding SSA emissions and their parameterization in climate models. Including a temperature dependence in SSA parameterizations can play a large role in the climate feedback, but further investigation is needed.

Plain Language Summary Atmospheric aerosols can have a cooling influence on Earth's climate by scattering sunlight and seeding cloud formation. Over oceans, aerosols often contain a high fraction of sea spray, and their abundance is strongly dependent on wind speed. High wind speeds cause wave breaking and bubble bursting, which emit sea spray aerosol (SSA). Previously SSA has been shown to have a cooling influence on surface climate. We show that when we artificially enhance SSA emissions in a coupled Earth system model that about half of the cooling influence is offset by the ocean response; more SSA emitted from the ocean leads to surface cooling, and therefore wind speeds weaken and produce less SSA. This is particularly important over the Southern Ocean which is the windiest region on Earth year-round. We show that, in a climate model, the strength of the feedback depends on how SSA emission is represented by the model. Therefore in a warmer, windier climate, simulating SSA accurately will be critical for understanding natural versus human influences on climate.

1. Introduction

Sea spray aerosol (SSA) is emitted from the world's oceans primarily at high wind speeds when waves break and bubbles burst. SSA has a cooling influence on climate via scattering of solar radiation—the direct aerosol effect—and via activation to cloud condensation nuclei (CCN) around which cloud droplets can form (Murphy et al., 1998). Clouds perturbed by aerosols tend to consist of more but smaller droplets and are optically brighter, therefore they scatter more solar radiation (Twomey, 1977) and may have a longer lifetime (Albrecht, 1989); together these comprise the indirect aerosol effect. Latham and Smith (1990) suggested that enhanced SSA fluxes would exert a negative climate feedback and, in a warmer windier climate, enhanced SSA concentrations could be "sufficient to compensate for predicted levels of global warming." Decades later, our understanding of how marine aerosol emissions and cloud formation will change as the world's oceans warm is still unclear (Brooks & Thornton, 2018; Quinn & Bates, 2011).

An important region of SSA production is the Southern Ocean, where wind speeds are high year-round, especially a region of peak westerly wind speed in the lower troposphere referred to as the midlatitude near-surface jet, or westerly jet, centered around 52°S (Karpechko & Maycock, 2018). The westerly jet affects Southern Hemisphere climate by influencing surface temperature and the variability of storm tracks (Thompson & Solomon, 2002; Yin, 2005). Between 1985 and 2018 near-surface (10 m) wind speeds across

the Southern Ocean increased by 6 cm s^{-1} $year^{-1}$ (Young & Ribal, 2019). In part, increasing wind speeds are due to stratospheric ozone depletion and the associated positive phase of the Southern Annular Mode (Son et al., 2008; Thompson & Solomon, 2002).

Numerous studies have documented the sensitivity of SSA production to wind speed (Gong, 2003; Grythe et al., 2014; Hartery et al., 2020; Jaeglé et al., 2011; Monahan et al., 1986). Korhonen et al. (2010) showed that increasing wind speeds between 50° and 65°S since the early 1980s increased SSA concentrations in the boundary layer, causing fractional increases in CCN similar in size (22%) as the reduction in CCN seen in the Northern Hemisphere over the same period resulting from air pollution mitigation. An analysis of SSA emissions in the Coupled Model Intercomparison Project (CMIP) phase 3 models showed that increases in the near-surface wind speed of 2% through the 21st century caused coarse-mode SSA to increase by 6%–18% over the Southern Ocean (Struthers et al., 2013).

Previously, it was postulated that marine phytoplankton could regulate climate via a feedback involving dimethyl sulfide (DMS), activation of DMS-derived sulfate aerosol to CCN and cascading effects on cloud albedo and sea surface temperature (SST)—the CLAW hypothesis (Charlson et al., 1987). However, the coupling between marine biogenic activity and CCN is not fully understood (Green & Hatton, 2014; Quinn & Bates, 2011). Here, we explore a proposed feedback involving SSA: Enhanced SSA fluxes (e.g., from marine cloud brightening strategies [Alterskjær et al., 2013; Kravitz et al., 2013]) could increase CCN and cloud albedo via the direct and indirect aerosol effects, similar to the CLAW hypothesis. Instead of considering the effects of changes in cloud albedo and SST on marine phytoplankton, we hypothesize that a SSA-induced decrease in incoming solar radiation (via the direct and indirect aerosol effects) would decrease SST. Since wind speeds over the Southern Ocean respond to changes in the meridional temperature gradient, a decrease in SST would reduce wind speeds and affect the position of the westerly jet. As a result, SSA fluxes at the latitude of the westerly jet would be suppressed, forming a negative feedback between the ocean and atmosphere.

2. Computational Methods

Simulations were performed with a coupled model, the United Kingdom Earth System Model UKESM1 (Sellar et al., 2019), and an atmosphere-only model, the Hadley Centre Global Environmental Model HadGEM3-GA7.1 (Mulcahy et al., 2018; Walters et al., 2019). Both models have N96 horizontal resolution, corresponding to grid cells of 1.875° × 1.25° and 85 levels in the atmosphere between the surface and 85 km. The HadGEM3-GA7.1 configuration used here differs from the standard configuration in several ways as documented by Revell et al. (2019), and Southern Ocean aerosols in this configuration were evaluated in the same study. Essentially, the configuration is very similar to UKESM1's atmosphere model except that seasalt density is increased in UKESM1 compared with HadGEM3-GA7.1 which leads to higher SSA emissions in UKESM1 (Mulcahy et al., 2020). To account for this difference, we compare relative changes in pairs of simulations rather than absolute differences between the atmosphere-only and coupled models.

In both models, aerosol evolution, growth and deposition are handled with the Global Model of Aerosol Processes (GLOMAP-mode, Mann et al., 2010; Mulcahy et al., 2020). Sources of marine aerosol include SSA, DMS, and primary marine organic aerosol (PMOA). SSA emissions are calculated online via a wind-speed-dependent parameterization (Gong, 2003), hereafter G03 (Equation 1):

$$\frac{dF}{dr} = 1.373u_{10}^{3.41}r^{-A}(1 + 0.057r^{3.45}) \times 10^{1.607e^{-B^2}} \quad (1)$$

The exponential terms A and B are defined by Equations 2 and 3:

$$A = 4.7(1 + \Theta r)^{-0.017r^{-1.44}} \quad (2)$$

$$B = \frac{(0.433 - \log(r))}{0.433} \quad (3)$$

Table 1
Model Simulations Performed

Experiment name	Model	SSA scaling	SSA source function
A1_G03	Atmosphere-only	1	G03
A2_G03	Atmosphere-only	2	G03
A10_G03	Atmosphere-only	10	G03
C1_G03	Coupled	1	G03
C2_G03	Coupled	2	G03
C10_G03	Coupled	10	G03
A1_J11	Atmosphere-only	1	J11
A10_J11	Atmosphere-only	10	J11
C1_J11	Coupled	1	J11
C10_J11	Coupled	10	J11

Abbreviation: SSA, sea spray aerosol.

where r is the particle radius at a relative humidity of 80%, Θ is an adjustable parameter that controls the shape of the size distributions (set to 30 in this model), and u_{10} is the scalar horizontal wind speed at 10 m above the surface. SSA is emitted in the accumulation mode (particle radii 50–250 nm) and coarse mode (250–5,000 nm) (Mulcahy et al., 2020). Aerosol particles are activated into cloud droplets following the scheme of Abdul-Razzak and Ghan (2000). A complete description of how aerosol-cloud interactions are handled in the model is given by Mulcahy et al. (2018), Revell et al. (2019) and Mulcahy et al. (2020).

Greenhouse gas concentrations were based on observations. Emissions of NO_x, CO, and volatile organic compounds were prescribed based on the year 2000 (Lamarque et al., 2010). SSTs and sea ice concentrations were based on observations in the atmosphere-only model (Rayner et al., 2003) and were calculated online in the coupled model.

To test the model responses to SSA forcing, simulations were performed with the SSA flux multiplied by 2 and 10 (Table 1). The annual-mean increase in cloud droplet number concentration over the Southern Ocean is 26% when the SSA flux is doubled, and 141% when the SSA flux is multiplied by 10. In contrast, the "G4cdnc" experiment requested for GEOMIP requires the cloud droplet number concentration to be increased by 50% over the ocean (Kravitz et al., 2013). Therefore while perturbing the SSA flux by a factor of 10 is unrealistic, it could be considered as an extreme geoengineering scenario. Since the 2× scaling did not always yield a clear signal from noise in all variables examined we focus mostly on the 10× SSA simulations. These give a clear depiction of how the model responds to enhanced SSA, permitting the use of shorter simulations.

Simulations were started from a spun-up state in 1988 and ran until 1999. Southern Ocean SST decreased by 1.3 K over the first 7 years of the coupled simulation with perturbed SSA before stabilizing; hence only the last 3 years of all simulations were analyzed. Results were tested for statistical significance at the 95% confidence level using a *t*-test for independent samples. To justify the use of short 3 year simulations, we also examine the 1,100 year-long *piControl* UKESM1 simulation performed for CMIP6 (Eyring et al., 2016; Tang et al., 2019), which is useful for assessing natural variability in climate models (Parsons et al., 2020; Richter & Tokinaga, 2020). Figures S1 and S2 confirm that the magnitude of the simulated SST and wind speed response is outside the model's natural variability.

To test the sensitivity of our results to the choice of SSA source function and explore the impact of SST on SSA production, a set of simulations were performed using the source function of Jaeglé et al. (2011) (hereafter J11), which includes SST as input along with scalar wind speed (Equation 4):

$$\frac{dF}{dr} = (0.3 + 0.1 \times SST - 0.0076 \times SST^2 + 0.00021 \times SST^3)1.373u_{10}^{3.41}r^{-A}(1 + 0.057r^{3.45}) \times 10^{1.607e^{-B^2}} \quad (4)$$

Finally, radiative forcing (RF) was calculated as the difference in the top-of-atmosphere outgoing radiative flux between simulations with 1× and 10× SSA scaling (Equation 5). By convention, a negative ΔRF means that more radiation is leaving the atmosphere and implies surface cooling.

$$\Delta RF = -(\Delta SW + \Delta LW) \quad (5)$$

3. Results and Discussion

3.1. Coupled Atmosphere-Ocean SSA Feedback

Figure 1 shows changes over the Southern Ocean when the SSA flux is perturbed. We focus on austral winter, June to August (JJA), when the Antarctic ozone hole does not influence the westerly jet (Son et al., 2008) and aerosol over the Southern Ocean consists primarily of SSA rather than biogenic-derived sources such as DMS and PMOA (Revell et al., 2019). The greatest increase in SSA is observed south of Australia (Figures 1a

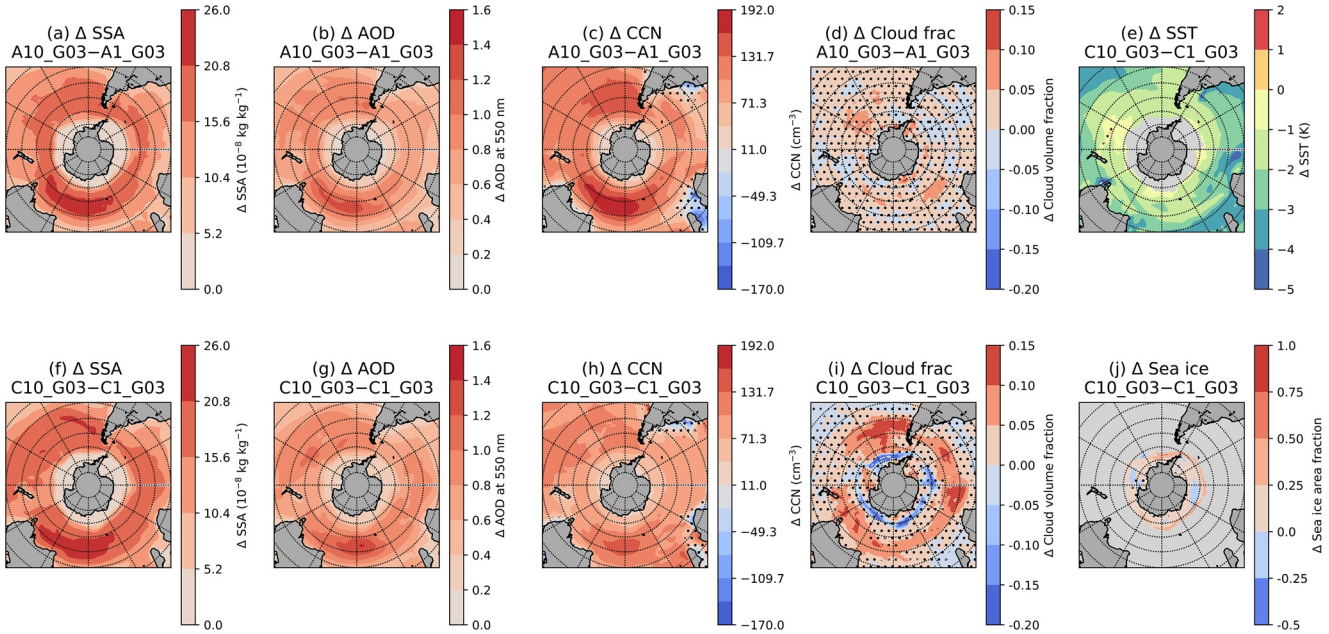

Figure 1. (a) Change in the surface SSA mass fraction in JJA in the A1_G03 and A10_G03 simulations (i.e., high minus low SSA). See Table 1 for experiment definitions. Stippling indicates that the difference is not statistically significant at the 95% level of confidence (independent *t*-test). (b) As for (a) but showing AOD. (c) CCN concentrations at 800 m (the approximate cloud base). (d) As for (a) but showing the cloud volume fraction at 800 m. (e) The change in SST in the coupled model simulations (C10_G03 minus C1_G03). (f–i): As for (a–d) but for coupled model simulations. (j) The change in sea ice area fraction in the coupled model simulations (C10_G03 minus C1_G03). AOD, aerosol optical depth; CCN, cloud condensation nuclei; JJA, June to August; SSA, sea spray aerosol.

and 1f) where the change in near-surface wind speed is greatest. A similar change is shown in aerosol optical depth (AOD; Figures 1b and 1g). Aerosol particles ≥50 nm in diameter can be "activated" to CCN around which water vapor can condense and cloud droplets form. Increases in CCN of up to 192 cm^{-3} can be seen in the atmosphere-only model when the SSA flux is scaled up by 10 (Figure 1c), while the coupled model shows a slightly smaller increase of 140 cm^{-3} (Figure 1h).

The cloud volume fraction increases by up to 0.10–0.15 over the Southern Ocean (Figures 1d and 1i). In the atmosphere-only simulation the increase is not statistically significant in most regions, although a clear increase between 40° and 50°S is seen in the coupled model simulation; likely as a result of cooler SSTs (Figure 1e). Increased scattering/reflection of incoming solar radiation by SSA leads to surface cooling in the coupled model of 1.7 K on average between 40° and 60°S (Figure 1e). In comparison, the JJA standard deviation typically does not exceed 0.5 K in the UKESM1 *piControl* simulation performed for CMIP6 (Figure S1), indicating that the magnitude of SST change shown in Figure 1e falls outside the model's internal variability over the Southern Ocean. Furthermore, the global-mean interannual variation in SST is typically much smaller; on the order of 0.2 K (Kuhlbrodt et al., 2018).

SST and sea ice changes are only shown for the coupled model since SST and sea ice are prescribed in the atmosphere model. A region of decreased cloud volume fraction is seen at approximately 60°S in the coupled model (Figure 1i), which is spatially correlated with an increase in the sea ice area fraction (Figure 1j). Antarctic sea ice forms mostly around the coast but is then blown north, leaving open water that freezes to form new ice (Weeks, 2010). Therefore, cooler SSTs may influence sea ice extent not just by promoting more freezing, but also by inhibiting melting at the northern extent. Increased sea ice cover implies reduced exchange of water vapor and heat between the air and ocean (Abe et al., 2016), leading to the reduced cloud cover shown by the coupled model at 60°S. In polar regions, sublimation of saline blowing snow over sea ice at high wind speeds may also be an important source of SSA (Huang et al., 2018). Blowing snow is not implemented in our model so is not represented here, but may lead to enhanced SSA concentrations over regions of increased sea ice in the real world.

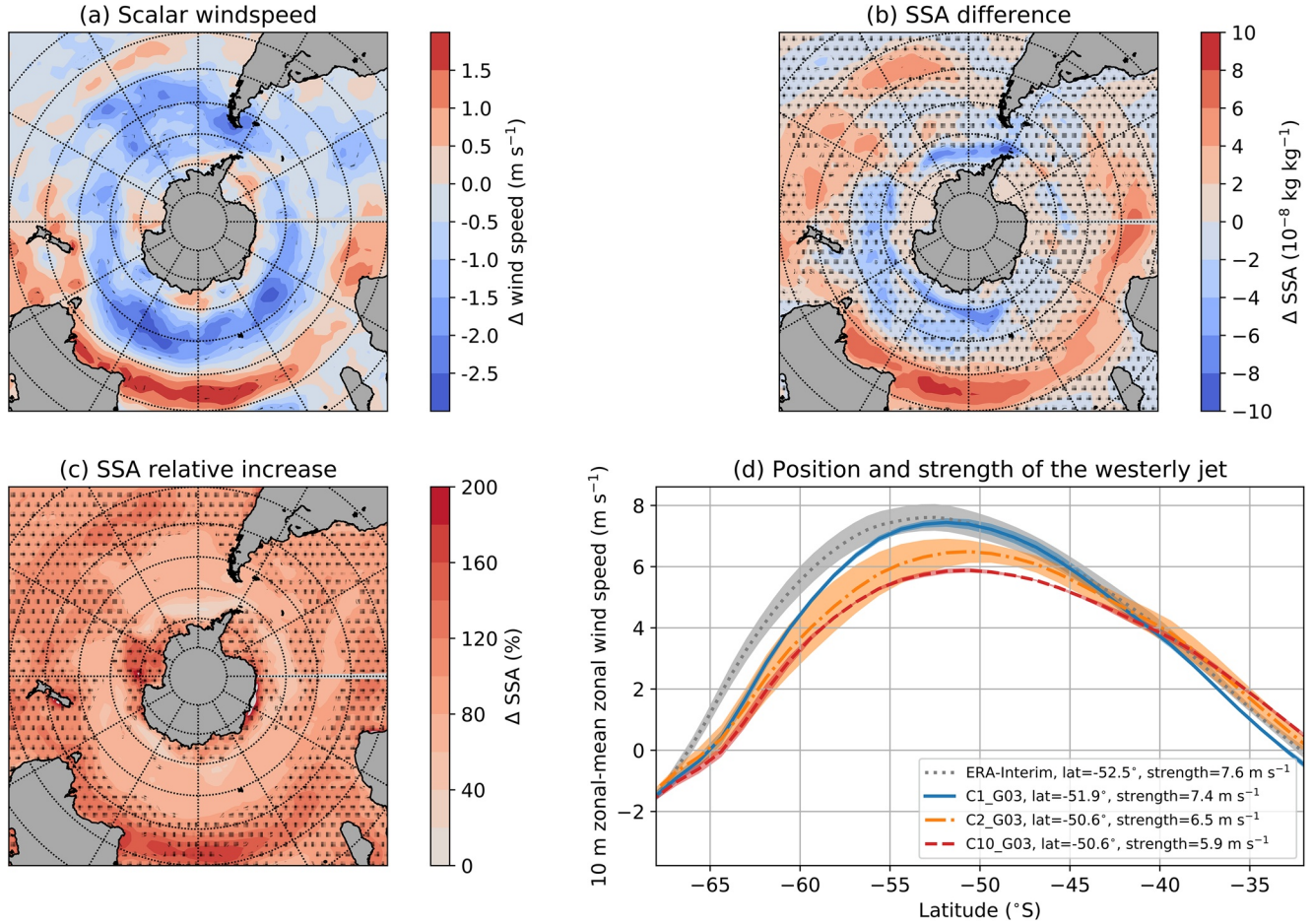

Figure 2. (a) The difference in the change in 10 m scalar wind speed in JJA when SSA is perturbed in the atmosphere-only and coupled simulations: (C10_G03−C1_G03) minus (A10_G03−A1_G03). Stippling indicates that the difference is not statistically significant at the 95% level of confidence (independent t-test). (b) As for (a), but showing the surface SSA mass fraction. (c) The relative increase in the surface SSA mass fraction in the coupled simulations (C10_G03−C1_G03) compared with the atmosphere-only simulations (A10_G03−A1_G03). (d) The annual-mean 10 m zonal-mean zonal wind speed. Shading indicates the 1σ standard deviation either side of the annual mean. JJA, June to August; SSA, sea spray aerosol.

We now compare the response of wind speeds and SSA concentrations to increased SSA forcing in the coupled and atmosphere-only model. The difference in the near-surface wind speed change in these simulations is shown in Figure 2a. The change in the scalar wind speed is weaker in the coupled model than in the atmosphere-only model by up to ~2.5 m s^{-1} at 50°S. Between 30° and 40°S the change is ~1.5 m s^{-1} larger in the coupled model than in the atmosphere-only model, but it is not always statistically significant at the 95% level of confidence. Shifts in wind speed patterns affect SSA production as shown in Figure 2b, because the SSA flux is parameterized in the model only as a function of wind speed (Equation 1). Larger surface SSA concentrations are simulated between 30° and 40°S when SSA is perturbed in the coupled model compared with the atmosphere-only model due to the region of maximum wind speed moving equatorward.

The SSA feedback dominates over the Southern Ocean (Figure S3), which is where wind speeds are highest year-round. Figure 2c indicates the strength of the feedback; on average, between 40° and 60°S, the increase in SSA in the coupled model is 72% of the increase in SSA in the atmosphere-only model. For the 2× SSA simulations, the increase in SSA over the Southern Ocean is 80% that simulated by the atmosphere-only model (not shown).

The westerly jet position and strength in the model is compared with the ERA-Interim reanalysis (Dee et al., 2011) in Figure 2d. The C1_G03 reference simulation agrees with ERA-Interim within ±1σ in the

region of maximum westerly wind speed (45°–55°S). Lower SSTs resulting from increased SSA forcing means that the westerly jet weakens and shifts equatorward in the C2_G03 and C10_G03 simulations.

As mentioned in Section 1, the atmosphere-ocean feedback in SSA discussed here is analogous in some respects to the CLAW hypothesis (Charlson et al., 1987). The main difference is that we are interested in the effect of SST on winds and wind-driven aerosol production, rather than the effect of SST and cloud albedo on marine biogenic activity and the production of DMS precursors. We deliberately focus on the JJA period as this is when DMS and PMOA concentrations are at their minimum (e.g., Mahajan et al., 2015; Mulcahy et al., 2020). It is expected that the SSA feedback may interact with emissions of DMS and PMOA and related climate feedbacks, for example through changes in SST and wind speed. We anticipate that the effects would be additive rather than contradictory, although non-linear interactions between sea spray and sulfate aerosol may occur (Fossum et al., 2020) and should be investigated in future studies.

3.2. Testing the SSA Feedback With an Alternative SSA Source Function

We have shown that perturbing the SSA flux leads to different results in the coupled and atmosphere-only simulations because of differences in simulated wind speed (related to the ocean response to atmospheric SSA forcing shown in Figure 1). The SSA source function used in our simulations is that of G03 and depends only on near-surface wind speed (Equation 1). However, SSA may also be influenced by SST via changes in the surface tension, density and viscosity of water (Grythe et al., 2014; Hartery et al., 2020; Jaeglé et al., 2011; Mårtensson et al., 2003; Ovadnevaite et al., 2014). To test the influence of including SST in the SSA source function, we performed simulations with the J11 source function (Equation 4).

AOD at 550 nm is shown for simulations performed with the G03 and J11 SSA source functions and compared with MODIS data in Figure S4. The model exhibits a wintertime bias in AOD over the Southern Ocean using the G03 SSA source function. This was also shown by Revell et al. (2019), who attributed the bias to overproduction of SSA via G03, since SSA is the dominant contributor to AOD over the Southern Ocean during JJA. Using the J11 source function, which is similar to G03 but with a SST term included (Equation 4), the wintertime bias is reduced over the Southern Ocean (Figure S4d).

We now examine how the SSA feedback changes when using the J11 SSA source function (Figure 3). With 10× SSA scaling, smaller changes are seen in the J11 coupled model simulations compared with the G03 simulations. There are two ways in which the J11 parameterization leads to a weaker feedback: first, the SSA flux is smaller in J11 compared with G03 over the Southern Ocean due to the SST dependency (Figure S4), so the magnitude of SSA forcing in the coupled model simulations is smaller. Second, it is apparent from Equation 4 that lower SSTs will act to weaken the SSA flux and hence weaken the strength of the atmosphere-ocean feedback.

Our results underline the need to understand the physical mechanisms underlying SSA emission. For example, while Equation 4 indicates that lower SSTs will weaken the SSA flux, Zábori et al. (2012) show that emission of SSA may increase at lower temperatures. J11 and Grythe et al. (2014) both discuss limitations in the mechanistic understanding of SST influences on SSA fluxes. Even if including SST in the SSA source function improves the present-day representation of aerosols, without a robust understanding of the underlying physical justification, climate models could give misleading results.

3.3. Changes in Radiative Forcing

Finally, to understand impact of perturbing SSA on radiative forcing over the Southern Ocean, top-of-atmosphere RF changes are shown in Table 2. The magnitude of outgoing radiation increases in all simulations when the SSA flux is perturbed (corresponding to a negative RF and therefore surface cooling), due to increased scattering and reflection of incoming solar radiation. From comparing the clear-sky and cloudy-sky ΔRFs, it can be seen that most of the change in SSA RF comes from the direct aerosol effect, rather than from indirect aerosol-cloud interactions, as the largest changes are seen in the clear-sky RFs. This is likely linked to the magnitude of SSA scaling applied in our perturbed simulations, but could also relate to how SSA is parameterized in the model; if too much SSA is emitted in the coarse mode, then it will be removed from the atmosphere rapidly and not act as an efficient CCN. The clear-sky ΔRF in the coupled

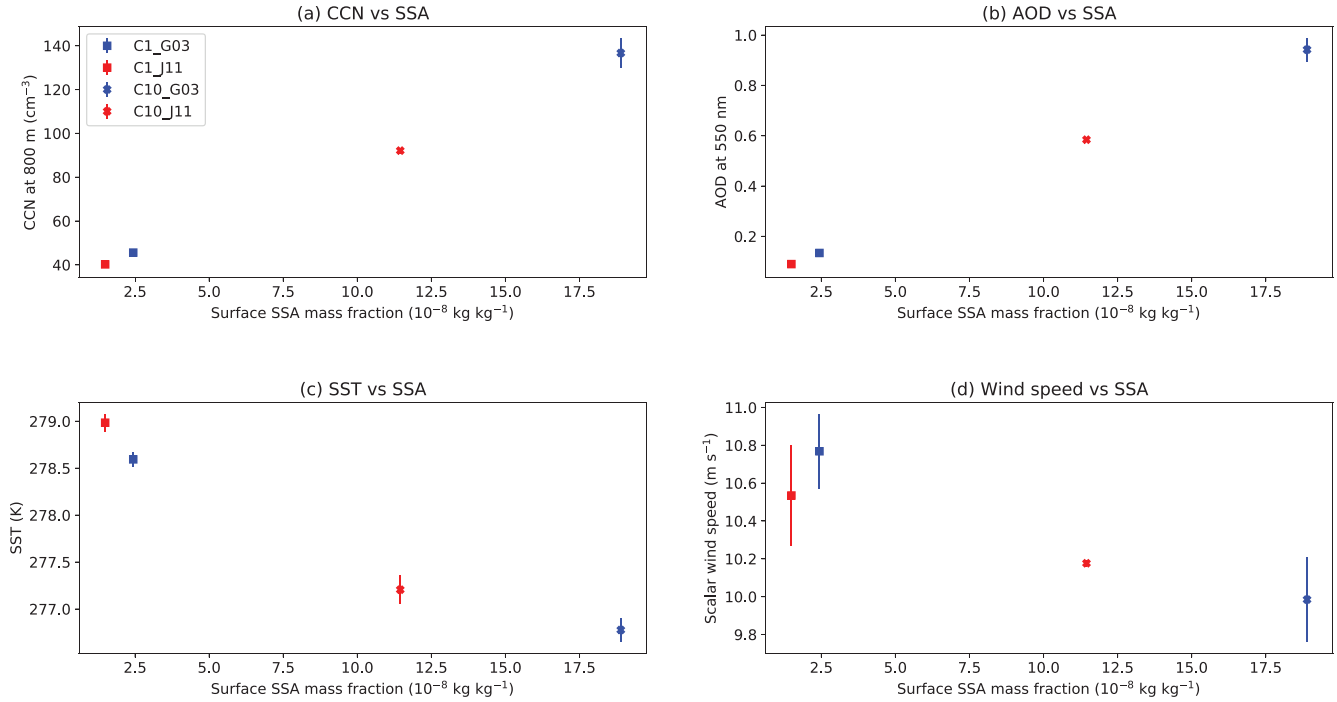

Figure 3. (a) CCN at 800 m versus the surface SSA mass fraction averaged over 40°–60°S for JJA. (b–d) show the same but for AOD, SST and scalar wind speed. Error bars indicate ±1σ either side of the JJA mean. AOD, aerosol optical depth; CCN, cloud condensation nuclei; JJA, June to August; SSA, sea spray aerosol.

G03 simulations (−1.79 W m^{-2}) is approximately one-quarter of that obtained with the atmosphere-only G03 simulations (−6.64 W m^{-2}) due to the moderating influence of the ocean on the SSA feedback.

This study focuses on rapid feedbacks between the atmosphere and ocean over a decade in response to SSA forcing. The long-term response is important too; it was recently shown that the dependence of SSA emissions on temperature can influence a model's equilibrium climate sensitivity (Paulot et al., 2020). Together with our results, this highlights the importance of parameterizing SSA accurately in climate models.

4. Conclusions

Comparing simulations performed with a coupled Earth System Model and an atmosphere-only model, we show the existence of a negative feedback in SSA production. Over the Southern Ocean where wind speeds and rates of wind-driven SSA production are high, enhanced SSA fluxes lead to cooling of the sea surface via scattering of incoming solar radiation and activation to CCN, which increases cloud cover. RF calculations indicate that the feedback is dominated by the direct aerosol effect. As a result of sea surface cooling, wind speeds decrease and SSA production is weakened. The increase in SSA concentration simulated by the coupled model during JJA is 72% that of the atmosphere-only model when the SSA emissions flux is artificially enhanced. The SSA feedback exists regardless of the SSA parameterization used, but is weaker when SST is included. The feedback in SSA production offsets approximately 20%–25% of the decrease in global-annual-mean RF when SSA forcing is enhanced.

We conclude that parameterizing SSA production correctly in climate models is vital for simulating future climate change. In particular, whether or not SST is included in the SSA parameterization could have significant implications. This is critical for the Southern Ocean, where climate model SST biases are primarily caused by atmospheric model net flux biases, meaning simulating clouds and aerosols correctly in this region is essential (Hyder et al., 2018). Finally, because enhanced SSA forcing

Table 2
Change in JJA Radiative Forcing Over the Southern Ocean, ΔRF (W m^{-2})

Comparison	Clear-sky	Cloudy-sky
A10_G03−A1_G03	−6.64	−2.54
C10_G03−C1_G03	−1.79	−2.77
A10_J11−A1_J11	−5.70	−1.77
C10_J11−C1_J11	−1.20	−1.93

Abbreviation: JJA, June to August.

weakens the Southern Hemisphere westerly jet and moves it equatorward, enhanced boundary layer aerosol concentrations—for example, from persistent wildfire smoke or marine cloud brightening geoengineering strategies—could also impact the position and strength of the westerly jet, which in turn influences Southern Hemisphere midlatitude climate.

Data Availability Statement

Model simulation data are accessible at: https://zenodo.org/record/4008715, https://doi.org/10.5281/zenodo.4008714.

Acknowledgments
The authors acknowledge the Deep South National Science Challenge for their support of this research (grant no. C01X1412) and the UK Met Office for the use of the MetUM. J. P. Mulcahy was supported by the Met Office Hadley Centre Climate Programme funded by BEIS and Defra (GA01101). The authors also wish to acknowledge the contribution of New Zealand eScience Infrastructure (NeSI) high-performance computing facilities to the results of this research. New Zealand's national facilities are provided by NeSI and funded jointly by NeSI's collaborator institutions and through the Ministry of Business, Innovation and Employment's Research Infrastructure programme (https://www.nesi.org.nz/, last access: 31 August 2020). The authors also acknowledge the MODIS mission scientists and associated NASA personnel for the production of data used in this research effort. Finally, the authors acknowledge the World Climate Research Programme, which, through its Working Group on Coupled Modelling, coordinated and promoted CMIP6. The authors thank the climate modeling groups for producing and making available their model output, the Earth System Grid Federation (ESGF) for archiving the data and providing access, and the multiple funding agencies who support CMIP6 and ESGF.

References

Abdul-Razzak, H., & Ghan, S. J. (2000). A parameterization of aerosol activation: 2. Multiple aerosol types. *Journal of Geophysical Research*, *105*(D5), 6837–6844. https://doi.org/10.1029/1999jd901161

Abe, M., Nozawa, T., Ogura, T., & Takata, K. (2016). Effect of retreating sea ice on arctic cloud cover in simulated recent global warming. *Atmospheric Chemistry and Physics*, *16*(22), 14343–14356. https://doi.org/10.5194/acp-16-14343-2016

Albrecht, B. A. (1989). Aerosols, cloud microphysics, and fractional cloudiness. *Science*, *245*(4923), 1227–1230. https://doi.org/10.1126/science.245.4923.1227

Alterskjær, K., Kristjánsson, J. E., Boucher, O., Muri, H., Niemeier, U., Schmidt, H., et al. (2013). Sea-salt injections into the low-latitude marine boundary layer: The transient response in three earth system models. *Journal of Geophysical Research: Atmospheres*, *118*(21), 12195–12206. https://doi.org/10.1002/2013jd020432

Brooks, S. D., & Thornton, D. C. O. (2018). Marine aerosols and clouds. *Annual Review of Marine Science*, *10*, 289–313. https://doi.org/10.1146/annurev-marine-121916-063148

Charlson, R. J., Lovelock, J. E., Andreae, M. O., & Warren, S. G. (1987). Oceanic phytoplankton, atmospheric sulphur, cloud albedo and climate. *Nature*, *326*(6114), 655–661. https://doi.org/10.1038/326655a0

Dee, D. P., Uppala, S. M., Simmons, A. J., Berrisford, P., Poli, P., Kobayashi, S., et al. (2011). The era-interim reanalysis: Configuration and performance of the data assimilation system. *Quarterly Journal of the Royal Meteorological Society*, *137*, 553–597. https://doi.org/10.1002/qj.828

Eyring, V., Bony, S., Meehl, G. A., Senior, C. A., Stevens, B., Stouffer, R. J., & Taylor, K. E. (2016). Overview of the coupled model intercomparison project phase 6 (CMIP6) experimental design and organization. *Geoscientific Model Development*, *9*(5), 1937–1958. https://doi.org/10.5194/gmd-9-1937-2016

Fossum, K. N., Ovadnevaite, J., Ceburnis, D., Preißler, J., Snider, J. R., Huang, R.-J., et al. (2020). Sea-spray regulates sulfate cloud droplet activation over oceans. *npj Climate and Atmospheric Science*, *3*(1), 14. https://doi.org/10.1038/s41612-020-0116-2

Gong, S. L. (2003). A parameterization of sea-salt aerosol source function for sub- and super-micron particles. *Global Biogeochemical Cycles*, *17*(4). https://doi.org/10.1029/2003GB002079

Green, T. K., & Hatton, A. D. (2014). The claw hypothesis: A new perspective on the role of biogenic sulphur in the regulation of global climate. *Oceanography and Marine Biology: An Annual Review*, *52*, 315–336. https://doi.org/10.1201/b17143-7

Grythe, H., Ström, J., Krejci, R., Quinn, P., & Stohl, A. (2014). A review of sea-spray aerosol source functions using a large global set of sea salt aerosol concentration measurements. *Atmospheric Chemistry and Physics*, *14*(3), 1277–1297. https://doi.org/10.5194/acp-14-1277-2014

Hartery, S., Toohey, D., Revell, L., Sellegri, K., Kuma, P., Harvey, M., & McDonald, A. J. (2020). Constraining the surface flux of sea spray particles from the Southern Ocean. *Journal of Geophysical Research: Atmospheres*, *125*(4), e2019JD032026. https://doi.org/10.1029/2019jd032026

Huang, J., Jaeglé, L., & Shah, V. (2018). Using CALIOP to constrain blowing snow emissions of sea salt aerosols over Arctic and Antarctic sea ice. *Atmospheric Chemistry and Physics*, *18*(22), 16253–16269. https://doi.org/10.5194/acp-18-16253-2018

Hyder, P., Edwards, J. M., Allan, R. P., Hewitt, H. T., Bracegirdle, T. J., Gregory, J. M., et al. (2018). Critical Southern Ocean climate model biases traced to atmospheric model cloud errors. *Nature Communications*, *9*(1), 3625. https://doi.org/10.1038/s41467-018-05634-2

Jaeglé, L., Quinn, P. K., Bates, T. S., Alexander, B., & Lin, J.-T. (2011). Global distribution of sea salt aerosols: New constraints from in situ and remote sensing observations. *Atmospheric Chemistry and Physics*, *11*(7), 3137–3157. https://doi.org/10.5194/acp-11-3137-2011

Karpechko, A., & Maycock, A. (2018). *Stratospheric ozone changes and climate* (Scientific assessment of ozone depletion: 2018WMO Global Ozone Res. Monit. Proj.—Rep. 58, Chap. 5). Geneva, Switzerland: World Meteorological Organization.

Korhonen, H., Carslaw, K. S., Forster, P. M., Mikkonen, S., Gordon, N. D., & Kokkola, H. (2010). Aerosol climate feedback due to decadal increases in Southern Hemisphere wind speeds. *Geophysical Research Letters*, *37*(2). https://doi.org/10.1029/2009gl041320

Kravitz, B., Forster, P. M., Jones, A., Robock, A., Alterskjaer, K., Boucher, O., et al. (2013). Sea spray geoengineering experiments in the geoengineering model intercomparison project (GeoMIP): Experimental design and preliminary results. *Journal of Geophysical Research: Atmospheres*, *118*(19), 11175–11186. https://doi.org/10.1002/jgrd.50856

Kuhlbrodt, T., Jones, C. G., Sellar, A., Storkey, D., Blockley, E., Stringer, M., et al. (2018). The Low-Resolution Version of HadGEM3 GC3.1: Development and Evaluation for Global Climate. *Journal of Advances in Modeling Earth Systems*, *10*(11), 2865–2888. https://doi.org/10.1029/2018ms001370

Lamarque, J.-F., Bond, T. C., Eyring, V., Granier, C., Heil, A., Klimont, Z., et al. (2010). Historical (1850-2000) gridded anthropogenic and biomass burning emissions of reactive gases and aerosols: Methodology and application. *Atmospheric Chemistry and Physics*, *10*(15), 7017–7039. https://doi.org/10.5194/acp-10-7017-2010

Latham, J., & Smith, M. H. (1990). Effect on global warming of wind-dependent aerosol generation at the ocean surface. *Nature*, *347*(6291), 372–373. https://doi.org/10.1038/347372a0

Mahajan, A. S., Fadnavis, S., Thomas, M. A., Pozzoli, L., Gupta, S., Royer, S.-J., et al. (2015). Quantifying the impacts of an updated global dimethyl sulfide climatology on cloud microphysics and aerosol radiative forcing. *Journal of Geophysical Research: Atmospheres*, *120*(6), 2524–2536. https://doi.org/10.1002/2014jd022687

Mann, G. W., Carslaw, K. S., Spracklen, D. V., Ridley, D. A., Manktelow, P. T., Chipperfield, M. P., et al. (2010). Description and evaluation of glomap-mode: A modal global aerosol microphysics model for the ukca composition-climate model. *Geoscientific Model Development*, *3*(2), 519–551. https://doi.org/10.5194/gmd-3-519-2010

Mårtensson, E. M., Nilsson, E. D., de Leeuw, G., Cohen, L. H., & Hansson, H.-C. (2003). Laboratory simulations and parameterization of the primary marine aerosol production. *Journal of Geophysical Research*, *108*(D9). https://doi.org/10.1029/2002jd002263

Monahan, E. C., Spiel, D. E., & Davidson, K. L. (1986). A model of marine aerosol generation via whitecaps and wave disruption. In E. Monahan, & G. M. Niocaill (Eds.), *Oceanic whitecaps* (pp. 167–174). Norwell, Mass: D. Reidel.

Mulcahy, J. P., Johnson, C., Jones, C. G., Povey, A. C., Scott, C. E., Sellar, A., et al. (2020). Description and evaluation of aerosol in UKESM1 and HADGEM3-GC3.1 CMIP6 historical simulations. *Geoscientific Model Development*, *13*(12), 6383–6423. https://doi.org/10.5194/gmd-13-6383-2020

Mulcahy, J. P., Jones, C., Sellar, A., Johnson, B., Boutle, I. A., Jones, A., et al. (2018). Improved aerosol processes and effective radiative forcing in HADGEM3 and UKESM1. *Journal of Advances in Modeling Earth Systems*, *10*(11), 2786. https://doi.org/10.1029/2018MS001464

Murphy, D. M., Anderson, J. R., Quinn, P. K., McInnes, L. M., Brechtel, F. J., Kreidenweis, S. M., et al. (1998). Influence of sea-salt on aerosol radiative properties in the Southern Ocean marine boundary layer. *Nature*, *392*, 62. https://doi.org/10.1038/32138

Ovadnevaite, J., Manders, A., de Leeuw, G., Ceburnis, D., Monahan, C., Partanen, A.-I., et al. (2014). A sea spray aerosol flux parameterization encapsulating wave state. *Atmospheric Chemistry and Physics*, *14*(4), 1837–1852. https://doi.org/10.5194/acp-14-1837-2014

Parsons, L. A., Brennan, M. K., Wills, R. C. J., & Proistosescu, C. (2020). Magnitudes and spatial patterns of interdecadal temperature variability in CMIP6. *Geophysical Research Letters*, *47*(7), e2019GL086588. https://doi.org/10.1029/2019gl086588

Paulot, F., Paynter, D., Winton, M., Ginoux, P., Zhao, M., & Horowitz, L. W. (2020). Revisiting the impact of sea salt on climate sensitivity. *Geophysical Research Letters*, *47*(3), e2019GL085601. https://doi.org/10.1029/2019gl085601

Quinn, P. K., & Bates, T. S. (2011). The case against climate regulation via oceanic phytoplankton sulphur emissions. *Nature*, *480*(7375), 51–56. https://doi.org/10.1038/nature10580

Rayner, N. A., Parker, D. E., Horton, E. B., Folland, C. K., Alexander, L. V., Rowell, D. P., et al. (2003). Global analyses of sea surface temperature, sea ice, and night marine air temperature since the late nineteenth century. *Journal of Geophysical Research*, *108*(D14). https://doi.org/10.1029/2002JD002670

Revell, L. E., Kremser, S., Hartery, S., Harvey, M., Mulcahy, J. P., Williams, J., et al. (2019). The sensitivity of Southern Ocean aerosols and cloud microphysics to sea spray and sulfate aerosol production in the HadGEM3-GA7.1 chemistry-climate model. *Atmospheric Chemistry and Physics*, *19*(24), 15447–15466. https://doi.org/10.5194/acp-19-15447-2019

Richter, I., & Tokinaga, H. (2020). An overview of the performance of CMIP6 models in the tropical Atlantic: Mean state, variability, and remote impacts. *Climate Dynamics*, *55*(9), 2579–2601. https://doi.org/10.1007/s00382-020-05409-w

Sellar, A. A., Jones, C. G., Mulcahy, J. P., Tang, Y., Yool, A., Wiltshire, A., et al. (2019). UKESM1: Description and evaluation of the UK earth system model. *Journal of Advances in Modeling Earth Systems*, *11*(12), 4513–4558. https://doi.org/10.1029/2019ms001739

Son, S.-W., Polvani, L. M., Waugh, D. W., Akiyoshi, H., Garcia, R., Kinnison, D., et al. (2008). The impact of stratospheric ozone recovery on the Southern Hemisphere westerly jet. *Science*, *320*(5882), 1486–1489. https://doi.org/10.1126/science.1155939

Struthers, H., Ekman, A. M. L., Glantz, P., Iversen, T., Kirkevåg, A., Seland, Ø., et al. (2013). Climate-induced changes in sea salt aerosol number emissions: 1870 to 2100. *Journal of Geophysical Research: Atmospheres*, *118*(2), 670–682. https://doi.org/10.1002/jgrd.50129

Tang, Y., Rumbold, S., Ellis, R., Kelley, D., Mulcahy, J., Sellar, A., et al. (2019). *MOHC UKESM1.0-ll model output prepared for CMIP6 CMIP picontrol*. Version = 20200617, Earth System Grid Federation. https://doi.org/10.22033/ESGF/CMIP6.6298

Thompson, D. W. J., & Solomon, S. (2002). Interpretation of recent Southern Hemisphere climate change. *Science*, *296*(5569), 895. https://doi.org/10.1126/science.1069270

Twomey, S. (1977). The influence of pollution on the shortwave albedo of clouds. *Journal of the Atmospheric Sciences*, *34*(7), 1149–1152. https://doi.org/10.1175/1520-0469(1977)034⟨1149:TIOPOT⟩2.0.CO;2

Walters, D., Baran, A. J., Boutle, I., Brooks, M., Earnshaw, P., Edwards, J., et al. (2019). The Met Office Unified Model Global Atmosphere 7.0/7.1 and JULES Global Land 7.0 configurations. *Geoscientific Model Development*, *12*(5), 1909–1963. https://doi.org/10.5194/gmd-12-1909-2019

Weeks, W. (2010). *On sea ice*. University of Alaska Press. Retrieved from https://books.google.co.nz/books?id=9S55O6WzuL8C

Yin, J. H. (2005). A consistent poleward shift of the storm tracks in simulations of 21st century climate. *Geophysical Research Letters*, *32*(18). https://doi.org/10.1029/2005gl023684

Young, I. R., & Ribal, A. (2019). Multiplatform evaluation of global trends in wind speed and wave height. *Science*, *364*(6440), 548–552. https://doi.org/10.1126/science.aav9527

Zábori, J., Krejci, R., Ekman, A. M. L., Mårtensson, E. M., Ström, J., de Leeuw, G., & Nilsson, E. D. (2012). Wintertime Arctic Ocean sea water properties and primary marine aerosol concentrations. *Atmospheric Chemistry and Physics*, *12*(21), 10405–10421. https://doi.org/10.5194/acp-12-10405-2012

References From the Supporting Information

Platnick, S., King, M. D., Ackerman, S. A., Menzel, W. P., Baum, B. A., Riedi, J. C., & Frey, R. A. (2003). The modis cloud products: Algorithms and examples from terra. *IEEE Transactions on Geoscience and Remote Sensing*, *41*(2), 459–473. https://doi.org/10.1109/TGRS.2002.808301

Sayer, A. M., Munchak, L. A., Hsu, N. C., Levy, R. C., Bettenhausen, C., & Jeong, M.-J. (2014). MODIS Collection 6 aerosol products: Comparison between Aqua's e-Deep Blue, Dark Target, and "merged" data sets, and usage recommendations. *Journal of Geophysical Research: Atmospheres*, *119*(24), 13965–13989. https://doi.org/10.1002/2014jd022453